

Lawrence Berkeley National Laboratory

Lawrence Berkeley National Laboratory

Title

THE ROLE OF BUFFER GASES IN OPTOACOUSTIC SPECTROSCOPY

Permalink

<https://escholarship.org/uc/item/0gr276tk>

Author

Thomas III, L.J.

Publication Date

1977-11-01

0 0 0 0 4 9 0 1 4 1 5

UC-37
LBL-6864
Preprint
c.1

Submitted to Applied Physics Letters

RECEIVED
LAWRENCE
BERKELEY LABORATORY

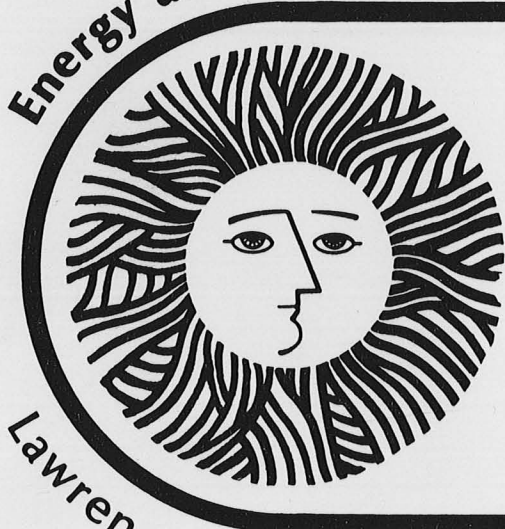
MAY 1 1978

LIBRARY AND
DOCUMENTS SECTION

For Reference

Not to be taken from this room

Energy and Environment Division



The Role of Buffer Gases in
Optoacoustic Spectroscopy

*Launey J. Thomas, III, Michael J. Kelly,
and Nabil M. Amer*

November 1977

Lawrence Berkeley Laboratory University of California/Berkeley

Prepared for the U.S. Department of Energy under Contract No. W-7405-ENG-48

37

LBL-6864
c.1

LEGAL NOTICE

This report was prepared as an account of work sponsored by the United States Government. Neither the United States nor the Department of Energy, nor any of their employees, nor any of their contractors, subcontractors, or their employees, makes any warranty, express or implied, or assumes any legal liability or responsibility for the accuracy, completeness or usefulness of any information, apparatus, product or process disclosed, or represents that its use would not infringe privately owned rights.

-iii-

The Role of Buffer Gases in
Optoacoustic Spectroscopy

Launey J. Thomas, III, Michael J. Kelly, and Nabil M. Amer

Physics Department
University of California, Berkeley
and
Applied Laser Spectroscopy Group
Lawrence Berkeley Laboratory
Berkeley, California 94720

ABSTRACT

The dependence of an acoustically resonant optoacoustic signal on the molecular weight, and thermodynamic and transport properties of the buffer gas is reported. Our results show that careful selection of such gases can significantly increase the sensitivity and flexibility of optoacoustic spectroscopy. We also demonstrate that such thermodynamic quantities as $\gamma (\equiv C_p/C_v)$ and sound velocity can now be measured readily and accurately. Other potential applications are suggested.

Little attention has been given to the role of a buffer gas (defined as the optically non-absorbing gaseous component in optoacoustic detectors) in optoacoustic spectroscopy. In principle, the molecular weight, and thermodynamic and transport properties of the buffer gas should have a significant impact upon the optoacoustic signal. One would also expect the energy transfer between the absorbing species and the buffer gas to play an important role in optoacoustic detection.

We have investigated the dependence of the optoacoustic signal on the following physical properties of the buffer gas: molecular weight and isotopic effects, heat capacity, thermal conductivity, and viscosity. In this letter we report our findings for acoustically resonant detectors. Results for the non-resonant case will be reported in a subsequent letter.

The following series of noble, diatomic, and polyatomic gases were investigated: Ne, Ar, Kr, Xe, N₂, CO, N₂O, ¹²CO₂, ¹³CO₂, and SF₆. The optically absorbing molecule in our case was CH₄ whose ν₃ absorption band lies conveniently in near coincidence with the 3.39 μm output of He-Ne lasers.

The experimental arrangement is shown in Fig. 1. A 3.39 μm beam from a Spectra-Physics model 124 He-Ne laser was intensity modulated by a continuously variable mechanical chopper. The acoustically resonant optoacoustic cell was a brass cylinder 10.8 cm in length and in diameter. NaCl flats were used as windows. A Knowles Electronics model BT-1759 miniature electret microphone (sensitivity 10 mV/Pa) with a built-in FET preamplifier was attached to the inner wall midway between the cell ends. The choice of a miniature microphone is particularly advantageous since

it can be readily incorporated in the resonant cavity without significantly degrading the Q of the resonances. Care was taken to insure mechanical and acoustical isolation of the detector. The noise level, which was electrical in origin, was found to be $\sim 90\text{nV/Hz}^{1/2}$. The gas temperature was monitored throughout the experiment.

In the case of a binary gas mixture, for a cylindrical cell the acoustic resonant frequencies are given by⁽¹⁾

$$f_{mnp} = \frac{\bar{v}_s}{2} \left[\left(\frac{\alpha_{mn}}{r} \right)^2 + \left(\frac{p}{\ell} \right)^2 \right]^{1/2} \quad (1)$$

where f_{mnp} is the frequency at which the acoustical modes occur. The eigenvalues m, n, and p refer to radial, azimuthal, and longitudinal modes, respectively; r is the radius and ℓ the length of the cavity, α_{mn} is the mth zero of the derivative of the Bessel function $dJ_n(\pi\alpha)/d\alpha$, and \bar{v}_s is the sound velocity in a mixture of ideal gases and is given by $\bar{v}_s = (\bar{\gamma} RT/M)^{1/2}$ where R is the ideal gas constant. We determined the effective specific heat ratio $\bar{\gamma}$ and the average molecular weight \bar{M} for the mixture from

$$\bar{\gamma} = \frac{x C_p^b + (1-x) C_p^a}{x C_v^b + (1-x) C_v^a} ; \quad \bar{M} = x M^b + (1-x) M^a$$

where C_p^b , C_v^b , C_p^a , and C_v^a are the heat capacities of the buffer and absorbing gases, respectively; M^b and M^a are their molecular weights; and x is the fractional concentration of the buffer gas.

From Eq. (1) it can be seen that the acoustic resonant frequencies are partially determined by the combined properties of the buffer and absorbing gases. In our case since $x \gg (1-x)$, the acoustical behavior of the cell will largely be determined by $\bar{\gamma}$ and \bar{M} of the buffer gas.

In Fig. (2) we show typical acoustical excitation spectra for pure CH_4 and for 0.9% CH_4 in N_2 and Xe, and in Table I we summarize our results. The agreement between the observed resonance frequencies and those calculated from Eq. (1) is excellent. Furthermore, our experimentally deduced velocity of sound for the different gases tested agrees to within $\leq 0.8\%$ of the calculated values. The discrepancy is attributable to uncertainties in the temperature and dimensions of the cell. As predicted, when the molecular weight of the buffer gas is increased, the resonance frequencies of the cavity shift to lower values.

In Table I we list the signal-to-noise ratio (S/N) as well as the experimentally and theoretically derived quality factor Q for different buffer gases. It can be seen that Xe enhances significantly the amplitude of the optoacoustic signal and yields the highest S/N observed. The largest experimental Q obtained was that of SF_6 , with CO_2 proving to be the most dissipative.

It should be noted that the amplitude of the optoacoustic signal is a function of: 1) the heat capacity of the mixture, 2) the laser power absorbed, 3) the modulation frequency, 4) the vibrational relaxation times of CH_4 , and 5) damping effects of the buffer gas. The first four contribute to the power going into the sound wave, and the last mechanism determines the Q of the resonances.

Assuming that boundary layer losses are the dominant dissipation mechanism, a theoretical Q can be obtained from^(2,3)

$$\frac{1}{Q} = \frac{1}{L} [d_v + (\bar{\gamma}-1) d_h (1 + \frac{l}{r})] \quad (2)$$

where the viscous boundary layer thickness $d_v = (2\eta/\rho\omega)^{\frac{1}{2}}$, the thermal boundary layer thickness $d_h = (2\kappa/\rho C_p \omega)^{\frac{1}{2}}$, η is the viscosity, κ the thermal conductivity, ρ the density of the gas mixture, and ω is the frequency.

Although it is not the purpose of this letter to fully account for the observed Q 's, the ratio $Q_{\text{exp}}/Q_{\text{cal}}$ is an indication of the relative significance of different energy dissipating mechanisms in the optoacoustic cavity. A value of unity for this ratio indicates that the viscous and thermal dissipations at the cell wall are the sole sources for sound energy loss. When $Q_{\text{exp}}/Q_{\text{cal}} < 1$, additional dissipating mechanisms have to be invoked in order to explain this discrepancy. For in the case of diatomic and polyatomic molecules, the energy losses due to shear friction and thermal diffusion are only part of the sound wave attenuating mechanism. One must, in addition, take into account the irreversible energy transfer from the sound wave to the internal degrees of freedom of the molecule; as a consequence, one would expect the characteristic relaxation times governing those transfer rates to affect the Q . Clearly, complete knowledge of the bulk relaxation times of the mixtures involved is necessary for understanding the role of molecular relaxation times in determining the Q . As to other loss mechanisms normally considered, e.g., Stokes-Kirchhoff losses, reflection, motion of microphone diaphragm, they can be shown to have negligible effect;^(2,3) while our Xe and SF₆ data limit the scattering contribution to <5%.

Typical resonant optoacoustic spectra contain three useful quantities: the frequency, the Q , and the amplitude of the signal. An illustration

of their utility is given in the following two examples:

1) It is of interest to investigate the ability of optoacoustic spectroscopy to mass-resolve⁽⁴⁾ two isotopes of the same molecular species. Figure (3) shows the acoustic signatures for the first radial mode of $^{12}\text{C } ^{16}\text{O}_2$ and $^{13}\text{C } ^{16}\text{O}_2$. As expected, due to the mass difference, the frequency of the (100) mode shifts from 3032 Hz to a lower value of 2994 Hz, which is in complete agreement with the theoretical prediction of Eq. (1).

2) To verify the sensitivity of our approach to differences in γ ⁽⁴⁾ when the molecular weight is very nearly identical, we determined the (100) resonance frequency for N_2O and $^{12}\text{CO}_2$ whose molecular weights are 44.013 and 44.010, and whose γ 's are 1.301 and 1.287, respectively. From Eq. (1) the first radial mode for N_2O and $^{12}\text{CO}_2$ should occur at 3009 and 3030 Hz, respectively. In Fig. (4) we present the experimental spectra which agree very well with the predicted values and which correspond to a difference of only 1.8 m/sec. in the sound velocity in the two gases.

The practical implications of our results are manifold. First, with respect to extending the flexibility and sensitivity of optoacoustic spectroscopy: we have shown that it is no longer necessary to limit the applicability of laser optoacoustic spectroscopy to species whose absorption must match available laser radiation. Instead, "doping" with a relatively small amount of an optically absorbing gas yields optoacoustic signatures of non-absorbing materials. We have also demonstrated that, for a fixed cavity dimension, the molecular weight of the buffer gas can serve as a means of shifting the frequency of the acoustical resonances

to any region of interest for the purpose of optimizing S/N; furthermore, irrespective of the frequency dependence on molecular weight, the use of such buffer gases as Xe enhances the sensitivity of optoacoustic detection. A consequence of both results is that, in the case where resonant optoacoustic detection is desirable, it now becomes possible to construct miniature resonance optoacoustic detectors by employing the appropriate high molecular weight buffer gas. Such a compact, room temperature detector can be of use in, for example, conventional and Fourier infrared spectroscopy and in gas chromatography-infrared analyzers.

Second, our findings point to the potential of this technique as a versatile analytical tool for "coarse" mass spectrometry and isotope analysis, for gas analysis, and for monitoring chemical reactions via changes in heat capacity and sound velocity.⁽⁵⁾

Finally, we have shown that quantities such as γ and v_s can now be measured readily by optoacoustic spectroscopy. In fact, we believe that we report the first experimentally deduced values for γ and v_s of $^{13}\text{CO}_2$ at 22.5°C. The values are 1.279 and 264.4 m/sec, respectively. It may also be possible to determine virial coefficients of gases by measuring the pressure dependence of sound velocity in high pressure optoacoustic cells.

Extensions of various aspects of this work are currently being pursued in our laboratory.

We thank D. Wake for technical assistance and H. Birecki, R. Gerlach, and T. Tyson for helpful discussions. This work was supported by the Department of Energy.

REFERENCES

1. P. M. Morse, Vibration and Sound. (McGraw-Hill, New York, 1948).
2. R. D. Kamm, J. Appl. Phys. 47, 3550 (1976).
3. P. M. Morse and K. U. Ingard, Theoretical Acoustics. (McGraw-Hill, New York, 1968); P. M. Morse and K. U. Ingard, in Handbuch der Physik, S. Flügge, Ed. (Springer-Verlag, New York, 1961), Vol. XI, Part 1.
4. Frequency resolution will depend on the linewidth of the resonance mode; i.e., the Q, which is gas dependent.
5. A. Einstein, Preuss. Akad. Wiss., Berlin, Ber., 24, 380 (1920).
6. K. Ražnjević, Handbook of Thermodynamic Tables and Charts. (McGraw-Hill, New York, 1976): JANAF Thermodynamical Tables. (U. S. Nat. Bur. Stand., NBS 37, 1971); J. C. McCoubrey and N. M. Singh, Trans. Farad. Soc. 53, 877 (1957).

Table I. Summary of Experimental Results^(a)

| Buffer Gas ^(b) | f_{100} (Hz) ^(c) | Q_{exp} ^(d) | $Q_{\text{exp}}/Q_{\text{cal}}$ | S/N |
|-------------------------------|-------------------------------|---------------------------------|---------------------------------|-------|
| Ne | 5074 | 554 | 0.56 | 3800 |
| Ar | 3619 | 694 | 0.62 | 6300 |
| Kr | 2495 | 832 | 0.86 | 11000 |
| Xe | 1995 | 903 | 0.95 | 14000 |
| CO | 3967 | 929 | 0.63 | 4900 |
| N ₂ | 3966 | 1030 | 0.71 | 5700 |
| ¹² CO ₂ | 3030 | 250 | 0.16 | 1400 |
| ¹³ CO ₂ | 2994 | 270 | -- | 1700 |
| N ₂ O | 3009 | 673 | 0.43 | 3300 |
| SF ₆ | 1522 | 1220 | 0.99 | 5500 |

- a. C_p , κ and η were obtained from Ref.6. f_{100} , Q_{exp} , $Q_{\text{exp}}/Q_{\text{cal}}$, and S/N for CH₄, without buffer gas, are 5033Hz, 500, 0.24, and 2800, respectively.
- b. Spectroscopic Grade.
- c. Typical uncertainty 1 Hz; f_{100} values agree to better than 0.8% with those calculated from Eq. (I).
- d. Q measured at half-power; typical uncertainty < 5%.

FIGURE CAPTIONS

Fig. (1). Schematic diagram of the experimental arrangement.

Fig. (2). Typical acoustically resonant optoacoustic spectra.

Fig. (3). First radial mode of the isotopically substituted pair $^{12}\text{CO}_2$
and $^{13}\text{CO}_2$.

Fig. (4). First radial mode of $^{12}\text{CO}_2$ and N_2O .

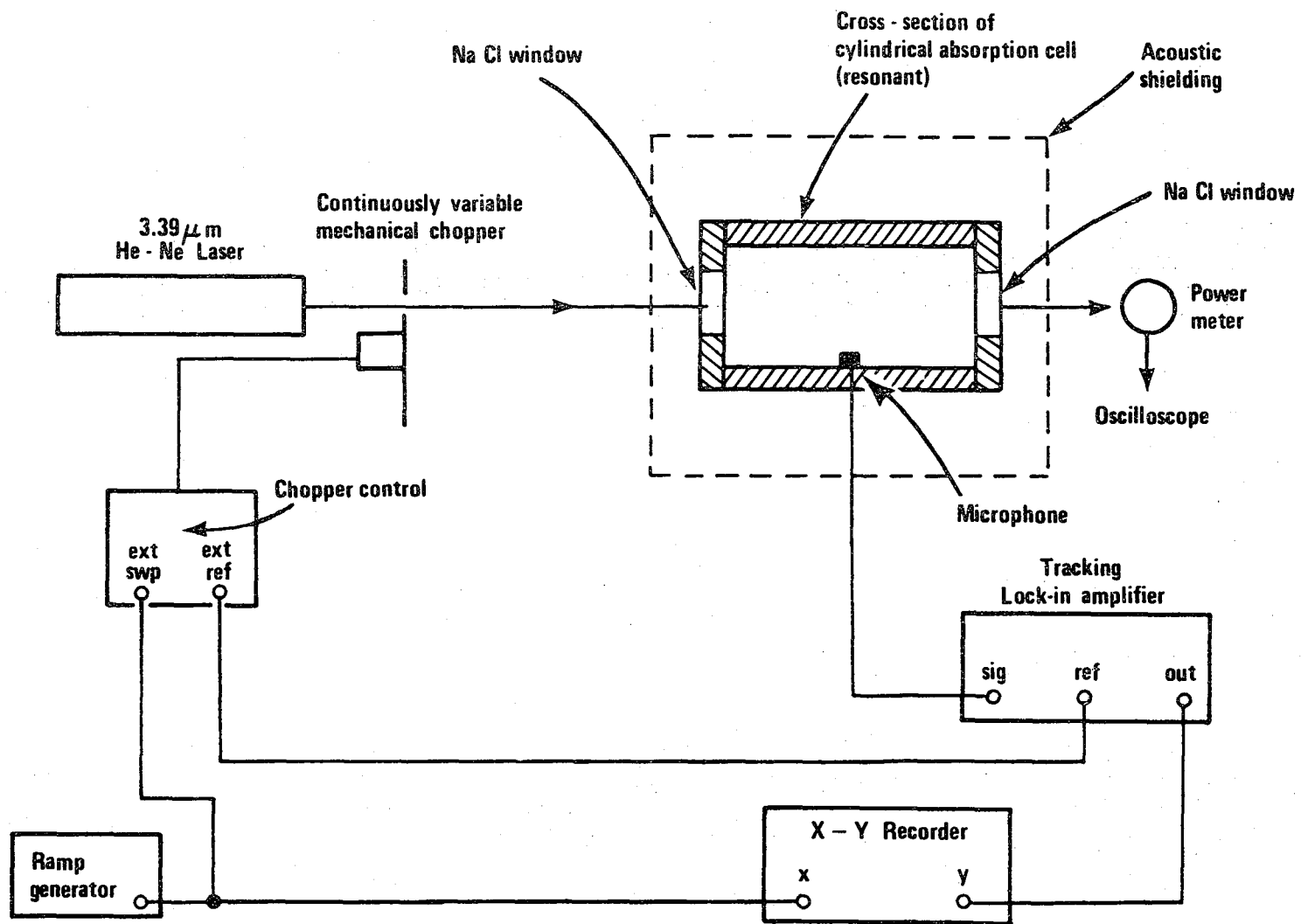
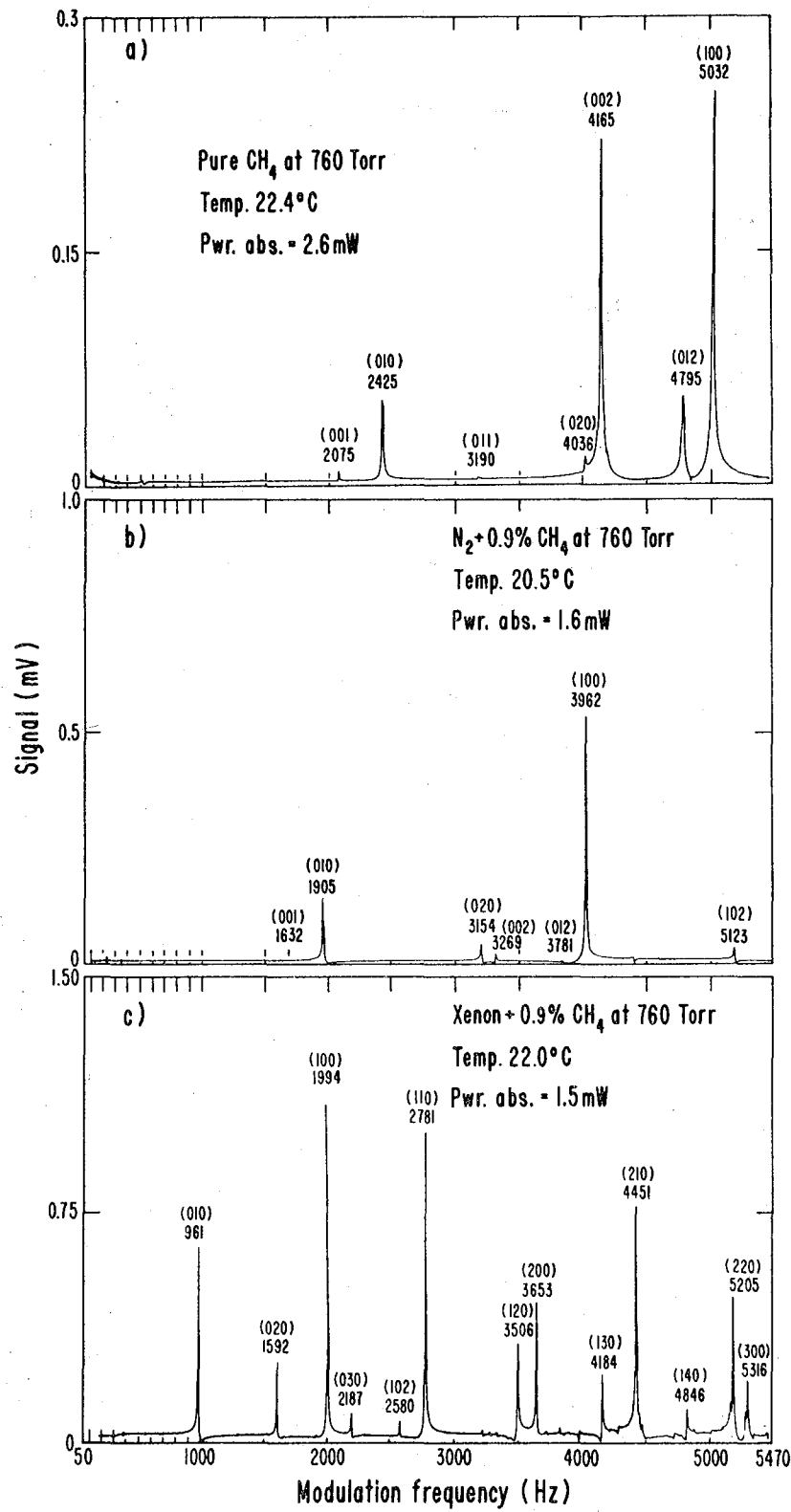


Fig. (1)

XBL 7710-2097 A



XBL 7710-2099

FIG. (2)

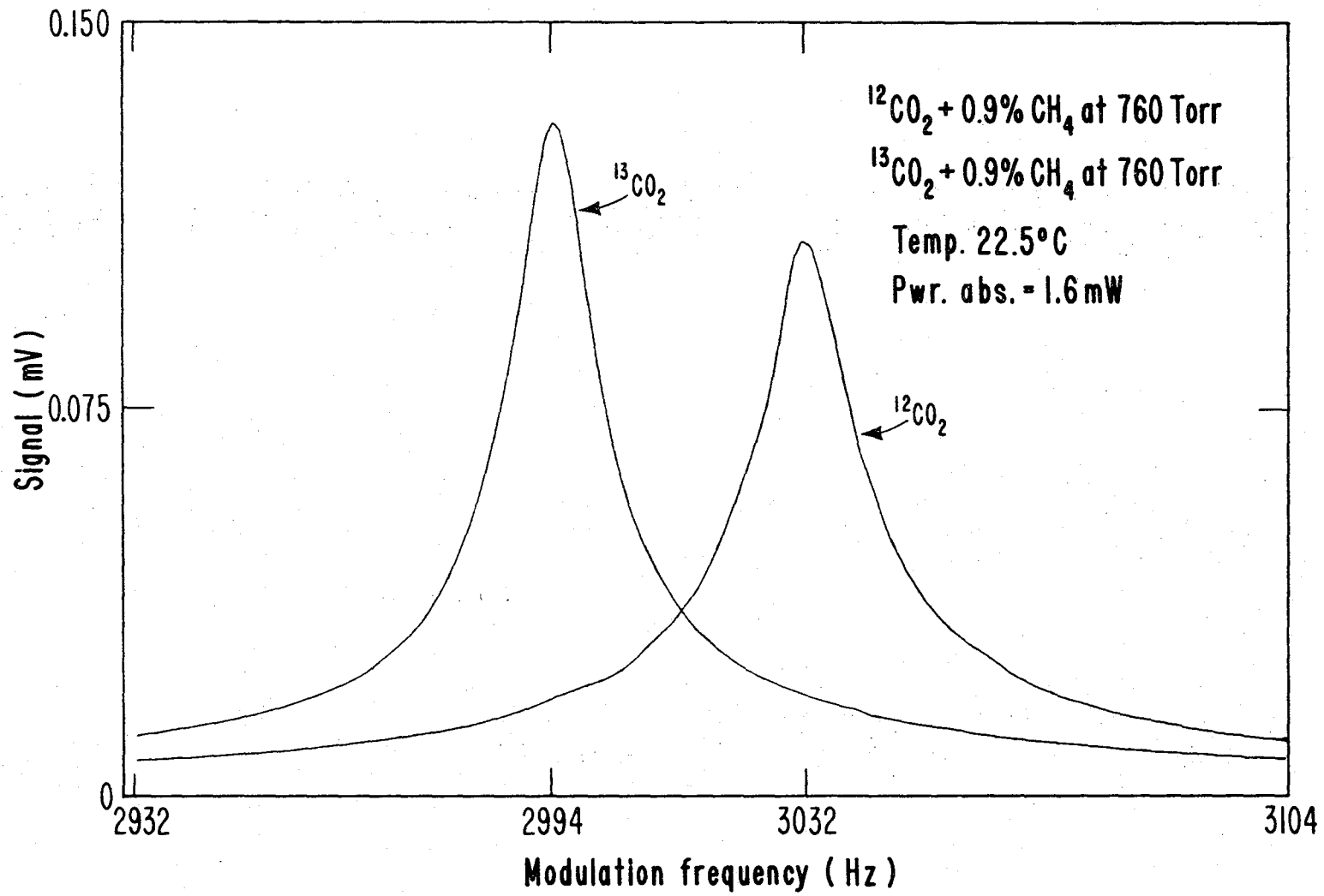
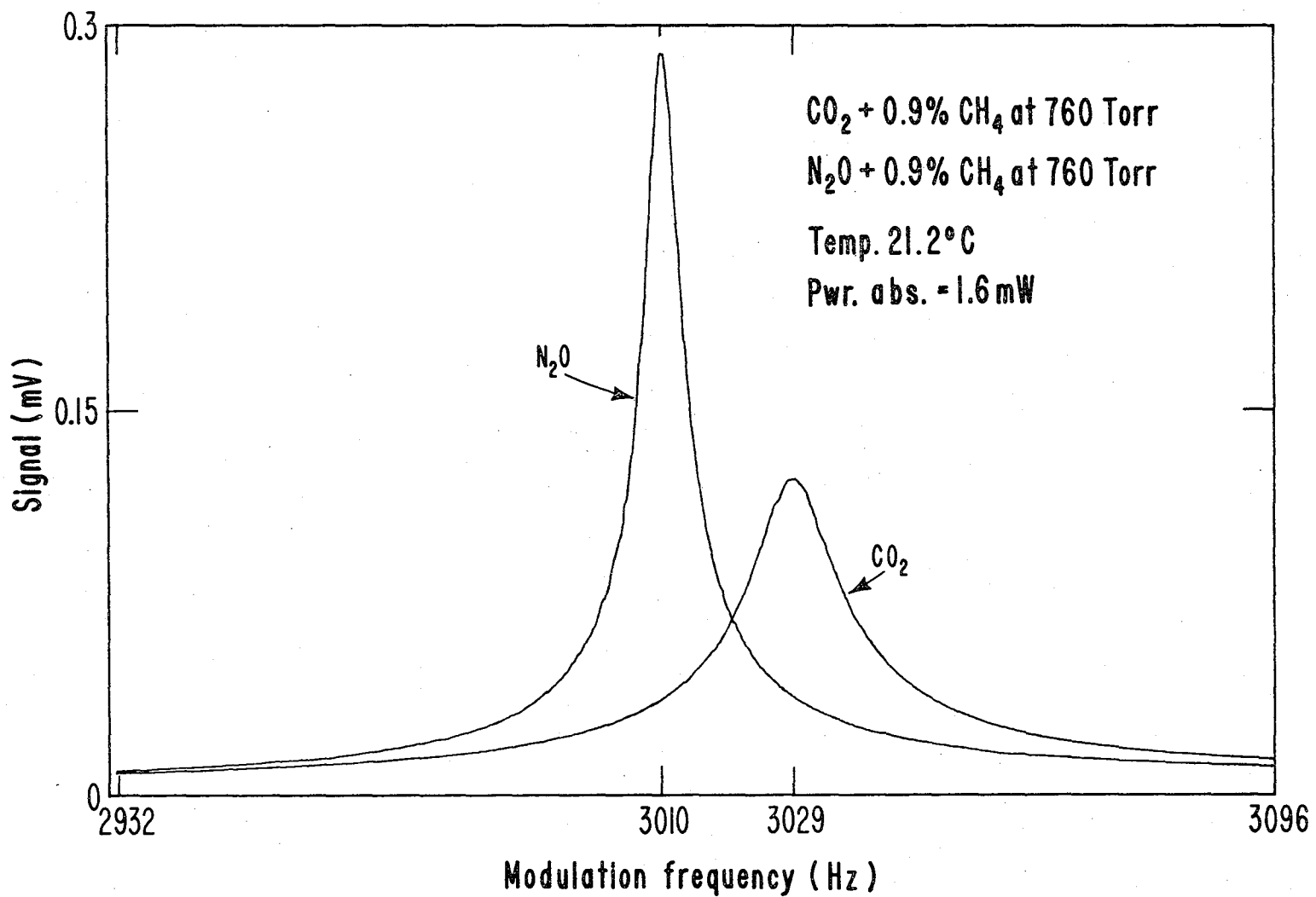


Fig. (3)

XBL 7710-2098



XBL 7710 - 2100

Fig. (4)

0000490-13-123

This report was done with support from the United States Energy Research and Development Administration. Any conclusions or opinions expressed in this report represent solely those of the author(s) and not necessarily those of The Regents of the University of California, the Lawrence Berkeley Laboratory or the United States Energy Research and Development Administration.